Laws controlling crystallization and melting in bulk polymers

Gert Strobl*

Physikalisches Institut, Albert-Ludwigs-Universität Freiburg, 79104 Freiburg, Germany.

After the fundamental structure of semicrystalline polymers - plate-like crystallites with thicknesses in the nanometer range being embedded in a liquid matrix - had been discovered in the late 1950s, attention turned to the mechanism of formation. After intense, controversial discussions an approach put forward by Hoffman and Lauritzen prevailed and was broadly accepted. The picture envisaged by the treatment - plate-like crystallites with atomically smooth side faces and a surface occupied by chain folds, growing side-ways layer by layer with a secondary nucleation as rate determining step - was easy to grasp and yielded simple relationships. The main control parameter is the supercooling below the equilibrium melting point of a macroscopic crystal, T_f^∞, which determines both the thickness of the crystallites and their lateral growth rate. The impression of many in the community that the mechanism of polymer crystallization is principally understood and the issue essentially settled however was wrong. Experiments carried out during the last decade on various polymer systems provided surprising new insights which are now completely changing the understanding. They revealed a number of laws which control polymer crystallization and melting in bulk, showing in particular that the crystal thickness is inversely proportional to the distance to a temperature T_c^∞ which is located above the equilibrium melting point and that crystal growth stops already at a temperature T_{zg} which is below T_f^∞. The observations indicate that the pathway followed in the growth of polymer crystallites includes an intermediate metastable phase. In a model proposed by us a thin layer with mesomorphic inner structure forms between the lateral crystal face and the melt. The first step in the growth process is an attachment of the coiled chain sequences of the melt onto the mesomorphic layer which subsequently is transformed into the crystalline state. The transitions between melt, mesomorphic layers and lamellar crystallites can be described with the aid of a temperature-thickness phase diagram. T_c^∞ and T_{zg} are identified with the temperatures of the (hidden) transitions between the mesomorphic and the crystalline phase, and between the liquid and the mesomorphic phase, respectively. Comparison of the predictions of the model theory with experimental results from small angle X-ray scattering, optical microscopy and calorimetry yields in addition to the three equilibrium transition temperatures latent heats of transition and surface free energies.

PACS numbers:

Contents

*Electronic address: `strobl@uni-freiburg.de`

I. INTRODUCTION

Considering that polymers are flexible long chains of coupled monomeric units one might have doubts at first, whether such objects can crystallize at all. In fact, this is possible, but occurs in a peculiar way (Strobl, 2007). In principle, a periodic structure in three dimensions can be obtained by choosing a unique helical conformation for all chains, orienting the helix axes parallel to each other and packing the chains in regular manner. However, for obvious reasons such an ideal crystal structure is never found. Starting from the melt where the chains are coiled and penetrate each other, this ideal state cannot be reached. This would require a complete disentangling of all the chains which needs a too long time. For about fifty years it has been known how nature deals with this situation, and Fig. 1 presents one of the electron micrographs obtained in this period. It shows the surface of a solid sample of polyethylene (PE). The picture resembles a landscape with many terraces. It represents an oblique cut through stacks of lamellar, i.e. plate-like, crystallites with curved edges. They have a lateral extension in the μm range and a thickness of about 20nm. Fig. 2 provides insight into the inner structure of the stacks. It shows an electron micrograph obtained for an ultrathin slice of polyethylene which was stained with OsO_4. Be-
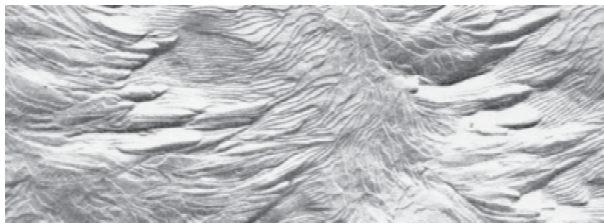
FIG. 1 Electron micrograph of a carbon film replica of a surface of PE (width of the depicted region: 5 μm). One observes stacks of plate-like crystallites with curved edges and a varying orientation on the sample surface. Picture obtained by Eppe and Fischer (Eppe *et al.*, 1959).
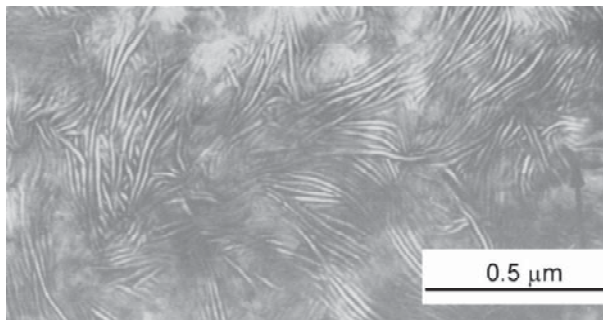

FIG. 2 Ultra-thin slice of a PE sample stained with OsO_4. The *bright* lines are crystalline lamellae of PE which are oriented edge-on, i.e., with the plate surface perpendicular to the surface of the slice. Crystallites are embedded in a *dark* fluid matrix. Electron micrograph obtained by Kanig (Kanig, 1975).

ing rejected by the crystallites the staining agent enters only regions which remained fluid. The contrast in the image then arises from the different absorption of the electron beam which is high in the stained, hence fluid parts. The white lines depict lamellar crystallites, but only those which stand up, i.e., are oriented with their layer plane perpendicular to the slice surface; then the electron beam can pass through with minor absorption. The two micrographs are typical and exemplify the basic structural principle in the morphology of polymeric solids: These are build up as a two phase structure, and are composed of plate-like crystallites that are separated by fluid regions. Cooling a melt to a temperature at which the polymer crystallizes results in a semicrystalline state with this character.

The development of such a structure is basically conceivable. Crystals of short-chain molecules like the *n*-alkanes are also composed of stacks of layers as is shown in the schematic drawing of Fig. 3 . The interfaces are occupied by the endgroups which cannot be incorporated in the interior parts of the layer. Similarly, polymer crystallization requires that one gets rid of the chain entanglements of the melt which cannot be resolved within the available short time. These are just shifted into the amor-

FIG. 3 Structure of a crystal of short-chain molecules like the *n*-alkanes. Schematic drawing with two layers. The layer thickness corresponds to the length of the molecules, the distance between neighbours is about 0.5 nm.

phous intercrystalline regions. Since the crystal thickness is small compared to the chain length, a given chain returns into the same or the adjacent crystal after an excursion into the amorphous region. For this reason the crystalline layers are since their first discovery named 'folded chain crystals'. The drawing in Fig. 4 pictures a section of such a polymer crystallite showing its interior with straight chain sequences and the two 'fold surfaces'.
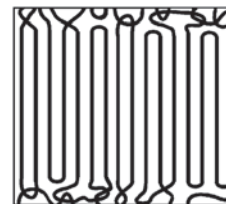

FIG. 4 Part of a lamellar crystallite in a semicrystalline polymer. Parallel straight chain sequences with a length of the order 10 nm set up the crystalline structure in the interior. The two surfaces, commonly addressed as 'fold surfaces', are occupied by sharp folds, loops, entanglements and other non-crystallizable chain parts.

The layer thickness depends on the crystallization temperature and generally increases with rising temperature.

When following the crystallization process in a polarizing optical microscope often growing spherulites are observed, as for example for the sample of poly(L-lactide) (PLLA) shown in Fig. 5 .The inner structure of

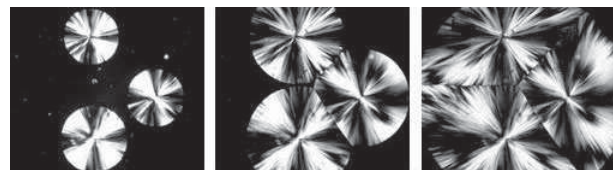FIG. 5 Growing spherulites observed during the crystallization of PLLA in a polarizing optical microscope. Image series obtained by Tai-Yon Cho, Universität Freiburg, 2006 .

these objects with sizes in the μm range is indicated in Fig. 6 together with an electron micrograph obtained for a spherulite of isotactic polystyrene (iPS). The structure results from a repeated branching and splaying of the
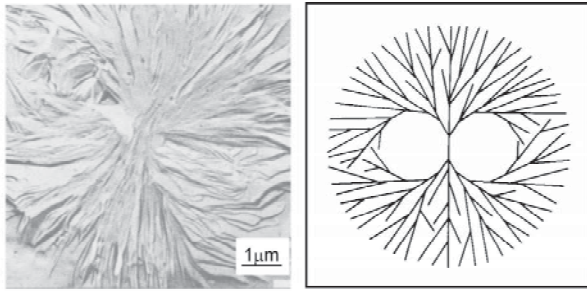
FIG. 6 Spherulite of iPS in an electron micrograph obtained by Vaughan and Bassett (Vaughan and Bassett, 1989). The orientation of the lamellar crystallites varies. Those in the central parts of the lower half are standing up, those in the lower right corner are lying flat(*left*). Schematic drawing showing the inner structure of a spherulite resulting from branching and splaying (*right*).

crystal lamellae. It implies that the radial growth rate of a spherulite is identical with the lateral growth rate of the constituent lamellar crystallites. In fact, polymer crystals grow in the two lateral directions only - growth in chain direction, i.e. normal to the plate surface, is blocked by the folds and loops. The growth rate varies with temperature in peculiar manner, exemplified by poly(ϵ-caprolactone) (PϵCL) in Fig. 7 : It decreases exponentially with rising temperature.
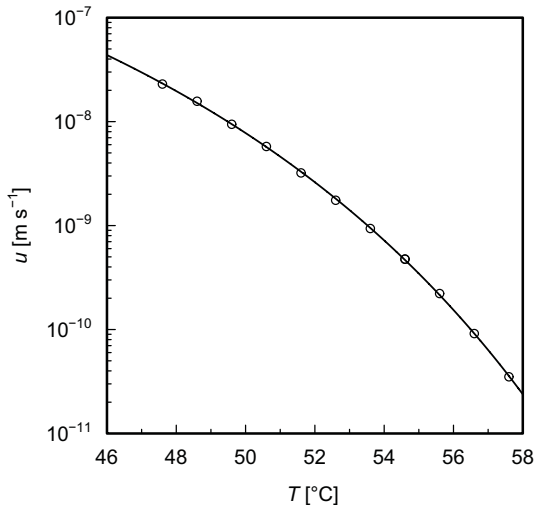

FIG. 7 Temperature dependence of the radial growth rate of spherulites of PϵCL (Cho *et al.*, 2007a).

When these basic properties of crystallizing polymers were revealed in the 1950s search for an understanding started immediately. Discussions concerned first of all the temperature dependent selection of the thickness of the lamellar crystallites and the mechanism of lateral crystal growth. Discussions were intense and a central topic in all structure oriented conferences in the

1960s and 1970s. One conference, organized as a Faraday Discussion 1979 in Cambridge, became famous as a climax (Faraday-Discussion, 1979). It brought together in often controversial discussions the different views and models developed by Fischer, Flory, Frank, Hoffman, Keller, Kovacs, Krimm, Point, Stein and Wunderlich, to cite only some of many prominent contributors. An agreement between the scientists could not be reached, neither at this conference nor afterwards. However, in the years which followed, one approach gained the ascendancy, and this was the one put forward by Hoffman, Lauritzen and their co-workers (Hoffman *et al.*, 1976). It was accepted and used in data evaluations by more and more workers, because the picture envisaged by the treatment was easy to grasp and the associated theory yielded simple equations for the lamellar thickness and the growth rate. The Hoffman-Lauritzen model was always accompanied by criticism, but this did not hinder its success. Some points were taken up and led to modifications, but the foundations remained unchanged. In the 1980s it developed into the 'standard model' of polymer crystallization and was broadly applied. The impression of many in the community that the mechanism of polymer crystallization is principally understood and the issue essentially settled was, however, wrong. With the 1990s a renewed thinking set in, triggered by new experimental results which contradicted the Hoffman-Lauritzen equations. It is now the common opinion of the majority of experts in the field that conventional wisdom is incorrect and needs a revision. The experimental evidence is clear, the interpretation is under discussion. We offered a new approach for the understanding.

To justify once again the necessity of a change in understanding we begin with a brief description of the previous conventional views (section II). Next the contradicting experimental results from the last decade are presented. They can be expressed by a set of laws which generally control crystallization and melting in polymeric systems (section III). We understand these laws as clear indication for an interference of a transient mesophase in the crystallization process and briefly explain in the final section (IV) the proposed 'multistage model'.

II. CONVENTIONAL VIEWS. THE HOFFMAN-LAURITZEN MODEL

It is a characteristic property of polymer crystallization that growth rates vary exponentially with temperature, both near the melting point where they decay as demonstrated by the example of Fig. 7 and also near the glass transition where they increase with rising temperature (this temperature range is not included in the figure). The behavior indicates control of the growth process by some activation steps. Near the glass transition they occur related to the diffusive motion of chain sequences which have to pass over intra- and intermolecular activation barriers. Barrier heights are essentially

constant so that the rates of jumps over the barriers increase with rising temperature. The conditions found in the high temperature range near the melting point are different. The slowing down of growth when the temperature goes up is indicative for an increase of the barrier height. The thickness of the lamellar crystallites generally increases when the crystallization temperature is raised. It was therefore an obvious idea to relate the two observations and to associate the increasing barrier height of the activation step with the increasing thickness of the growing crystallites. Hoffman and Lauritzen proposed the model sketched in Fig. 8 . The drawing,
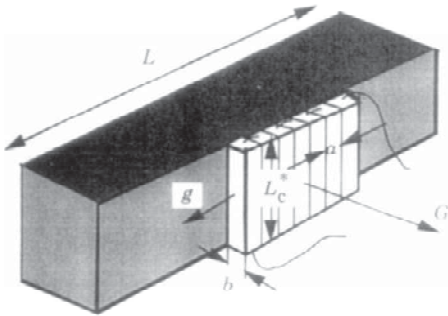

FIG. 8 Growth of a polymer crystallite as described by the Hoffman-Lauritzen model. The plate-like crystallite (fold surface in dark colour; the thickness here is denoted L_c^*, the width L is assumed as constant) extends in one lateral direction only with a growth rate G. The rate determining step is the formation of a secondary nucleus on the smooth growth face set up of refolded, repeatedly stretched chain sequences (folds connecting adjacent stems of stretched chain parts are indicated in the drawing). The attachment of further stems subsequent to the nucleation step (with rate g) is treated as a rapid process ($g \gg G$). From Hoffman, Davis and Lauritzen (Hoffman *et al.*, 1976).

reproduced from the original article, shows a lamellar crystallite which grows in one lateral direction only; the direction of growth is indicated by the vector G. It is assumed that the growth face (with normal vector parallel to G) is atomically smooth and that the rate determining step is the formation of a secondary nucleus created by an attachment of a refolded, repeatedly stretched chain sequence from the melt onto the growth face. When the nucleus has formed it expands rapidly into a monomolecular layer. The model thus has many features of the layer-by-layer growth mode of low molar mass crystals leading to a facetted shape. Based on this model Hoffman and Lauritzen analysed the growth kinetics, asking for the crystal thickness which would give the maximum growth rate. In fact, the semicrystalline state does not represent a thermal equilibrium associated with the Gibbs free energy minimum, but is kinetically determined, i.e., the developing structure is that with the maximum rate of formation. The theoretical treatment resulted in the conclusion that the maximum growth rate is achieved by crystallites whose thickness is near the stability limit, i.e. the melt-

ing point, of the lamellar crystallites. The melting point of a crystal with thickness d_c (in the drawing Fig. 8 the thickness is denoted L_c^*) is given by the Gibbs-Thomson equation, as

$$T(d_c) = T_f^\infty - \frac{2\sigma_e T_f^\infty}{\Delta h_f} \frac{1}{d_c} \quad . \tag{1}$$

The equation describes the suppression of the melting point below the equilibrium value of a macroscopic body, T_f^∞, caused by the excess free energy σ_e of the fold surface; Δh_f denotes the heat of fusion. For a crystallization temperature T the Hoffman-Lauritzen treatment predicted a thickness of the growing crystals of

$$d_c = \frac{2\sigma_e T_f^\infty}{\Delta h_f(T_f^\infty - T)} + \delta, \tag{2}$$

hence, a value inversely proportional to the supercooling below T_f^∞, apart from a minor excess δ necessary for providing a driving force. The associated growth rate u followed as

$$u = u_0 \exp\left(-\frac{T_A^*}{T}\right) \cdot \exp\left(-\frac{T_G}{T_f^\infty - T}\right) \quad . \tag{3}$$

The first exponential term expresses the temperature dependence of the segmental mobility in the melt; for temperatures above the glass transition it obeys an Arrhenius law with some effective activation temperature T_A^*. The second exponential term refers to the free energy of activation associated with the placement of a secondary nucleus on the growth face. It diverges together with d_c at T_f^∞. For the parameter T_G theory yielded an expression of the form

$$T_G = \frac{K}{T} \quad , \tag{4}$$

with K being determined by $\Delta h_f, \sigma_e$ and the surface free energy σ_l of the growth face.

The Hoffman-Lauritzen model was widely accepted. It became a standard procedure to evaluate growth rate data of polymer systems as suggested by the theory, and to derive from results surface free energies of the secondary nucleus.

III. NEW EXPERIMENTAL RESULTS

In the 1990s new ideas came up, triggered by new observations:

- Keller and his co-workers, when crystallizing polyethylene at elevated pressures, observed the formation of the orthorhombic crystals out of a disordered hexagonal phase and speculated that this may also happen under normal pressure conditions (Rastogi *et al.*, 1991) (Keller *et al.*, 1994).

- Kaji and co-workers interpreted a scattering of X-rays which they observed prior to the scattering by the crystallites as indicating the buildup of a precursor phase prior to the crystal formation (Imai *et al.*, 1995) , and Olmsted constructed a corresponding theory (Olmsted *et al.*, 1998).

- Temperature dependent small angle X-ray scattering (SAXS) experiments, at first carried out for syndiotactic (*s*-)polypropylene (sPP) and related octene copolymers (sPPcOx: chains include a fraction x of statistically distributed octene co-units), contradicted the basic assumption of a control of the lamellar thickness by the supercooling below the equilibrium melting point (Hauser *et al.*, 1998).

A. Crystallization line, recrystallization line and melting line

Considerations about mechanisms of crystallization and melting in polymers require as basic ingredients

- a knowledge of the variation of the crystal thickness, d_c, with the crystallization temperature,

- a monitoring of possible structure changes during a heating to the melting point, and

- a knowledge of the variation of the melting temperature with the crystal thickness.

During the development of the Hoffman-Lauritzen model the focus was mainly on growth rate measurements; temperature dependent studies of the lamellar structures were rare. With the aid of small angle X-ray scattering experiments employing appropriate efficient methods of data evaluation (Ruland, 1977) (Schmidtke *et al.*, 1997) it was possible to determine these structural properties, at first for *s*-polypropylene together with a variety of sPPcOs and then also for isotactic (*i*-)polypropylene (iPP), polyethylene together with octene copolymers (PEcOx), poly(ϵ-caprolactone), poly(L-lactide) and poly(1-butene) (Strobl, 2006). Figs. 9 and 10 present as two typical examples the results obtained for sPPcO15 (*s*-polypropylene with 15% of octene units) and poly(ϵ-caprolactone). As suggested by the Gibbs-Thomson equation, the melting points are plotted as a function of the inverse crystal thickness, d_c^{-1}, and the same representation is used here also for the relation between the crystallization temperature and the crystal thickness. The appearance of the plots is peculiar and typical for all investigated samples: Two straight lines are found that cross each other. The 'melting line', giving the dependence between the melting temperature and d_c^{-1}, agrees with the Gibbs-Thomson equation. This allows a determination of the equilibrium melting point T_f^∞ by a linear extrapolation to $d_c^{-1} = 0$. The 'crystallization line' gives the relationship between the crystallization temperature and d_c^{-1}. It has a higher slope than the melting line, intersects the latter at a finite value of
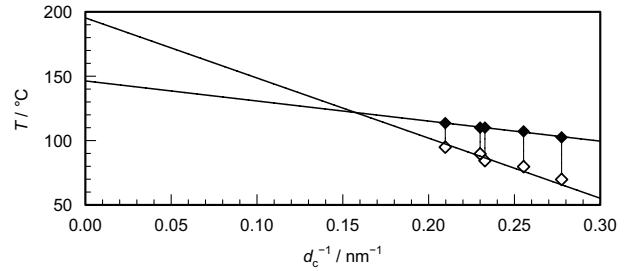

FIG. 9 sPPcO15, results of temperature dependent SAXS experiments: Crystallization line describing the relationship between the crystallization temperature T and the inverse crystal thickness d_c^{-1} (*open symbols*) and Gibbs-Thomson melting line giving the melting points T as a function of d_c^{-1} (*filled symbols*). The vertical direction of the connecting lines indicates that crystals have a constant thickness up to the melting point (Hauser *et al.*, 1998).
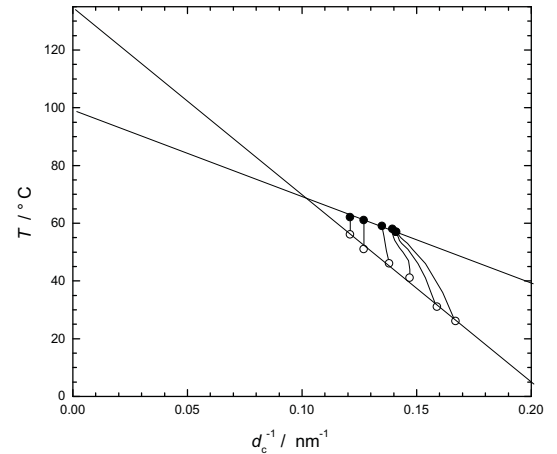

FIG. 10 PϵCL: Crystallization line and melting line. For crystallization temperatures below 40 °C crystals increase in thickness before the final melting (Heck *et al.*, 1999).

d_c^{-1} and has a limiting temperature for $d_c^{-1} \to 0$, denoted T_c^∞, which differs from T_f^∞. The crystallization line is described by

$$d_c^{-1} = C_c(T_c^\infty - T) \ . \tag{5}$$

The crossing implies $T_c^\infty > T_f^\infty$. The results of the temperature dependent measurements during heating are given by the thin lines which connect respective points on the crystallization line and the melting line. The lines are vertical when the thickness remains constant and are curved when the thickness increases during heating.

The existence of straight crystallization lines in all investigated systems expresses a first simple law: Crystal thicknesses are inversely proportional to the distance from a certain characteristic temperature, T_c^∞, which is different from the equilibrium melting point T_f^∞. In the two examples T_c^∞ is 35 °C and 50 °C above T_f^∞.

Lamellar crystallites can only exist at temperatures below the melting line. Therefore, crystals with thicknesses as given by the crystallization line cannot be formed any longer when the temperature of the intersection point is approached. This is indeed experimentally confirmed. Results of small angle X-ray scattering experiments in the interesting temperature range were obtained for sP-PcO20 and they are shown in Fig. 11 . Points deviate
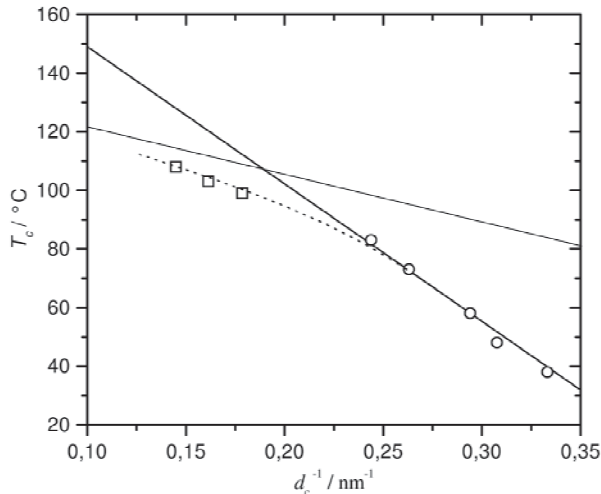

FIG. 11 sPPcO20: Relationship between crystallization temperature and crystal thickness in the range around the point of intersection between the melting line and the crystallization line. Crystallization at the three highest temperatures (*square symbols*) was carried out applying 'self-seeding' (Strobl, 2000).

from the crystallization line already before reaching the point of intersection. The results were obtained using a procedure known as 'self seeding' which greatly enhances the number of nuclei and thus allows observation of crystallization processes also at high temperatures. The enhancement is achieved by stopping a heating process immediately after the sample melting followed by a rapid cooling down to the crystallization temperature.

The presence of co-units (units with a different chemical structure) in a chain which cannot be included in the crystal lattice modifies the crystallization and melting properties. Temperature dependent small angle X-ray scattering studies were carried out to see these effects. The findings for *s*-polypropylene and a variety of different sPPcOs are depicted in Fig. 12 . Contrasting the normal behavior of the melting lines, which shift to lower temperatures when the co-unit content increases, the crystallization line is invariant within this set of samples. One observes a unique T vs d_c^{-1} relationship common to all of them, which determines d_c as being inversely proportional to the supercooling below $T_c^\infty = 195$ °C .

For the crystallization temperatures chosen in the experiments of Fig. 12 all crystallites keep their thickness constant up to the point of melting. A different behavior is observed when the crystallization is carried out at lower
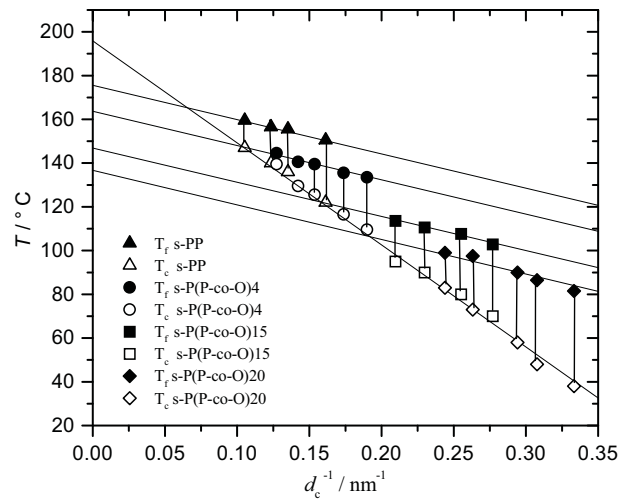

FIG. 12 sPP and sPPcOx: Unique crystallization line (*open symbols*) and series of melting lines (*filled symbols*). Extrapolation of the melting lines to $d_c^{-1} = 0$ yields the respective equilibrium melting points. They decrease with increasing co-unit content (Hauser *et al.*, 1998).

temperatures, down to temperatures near to the transition into the glassy state . When heating such a sample after the completion of the crystallization, reorganization processes set in. The crystal thickness generally increases upon heating, and this reorganization process proceeds continuously. Fig. 13 shows as an example the result of corresponding small angle X-ray scattering experiments on three different samples of *s*-polypropylene. Samples were isothermally crystallized and then heated stepwise. The figures present the variation of the thickness up to the melting point, again in plots of d_c^{-1} versus the temperature. All the initial points are located on the unique crystallization line of *s*-polypropylene. For crystallization temperatures in the low temperature region heating is accompanied by a continuous crystal thickening indicative for overall reorganization processes. Recrystallization goes on up to the temperature of final melting, indicated by a star. This temperature of final melting does not depend on initial crystallization temperature. In the case of sPPcO20 crystallized at 20 °C heating leaves the crystal thickness at first constant. This changes at 50 °C . Here thickening processes set in, and the further course is well defined: d_c^{-1} changes linearly with temperature following the drawn 'recrystallization line'. Recrystallization ends at 85 °C with the melting. The same dependence shows up when sPPcO20 is at first crystallized at 40 °C . Recrystallization again sets in when the recrystallization line is reached, and d_c^{-1} follows this line from thereon, up to the final melting. The line in the diagram guiding the process of recrystallization for sPPcO20 controls also the recrystallization for the other two samples. The line is equally included in all three figures in Fig. 13 . The recrystallization line has a characteristic property: Extrapolation of the line to $d_c^{-1} \to 0$
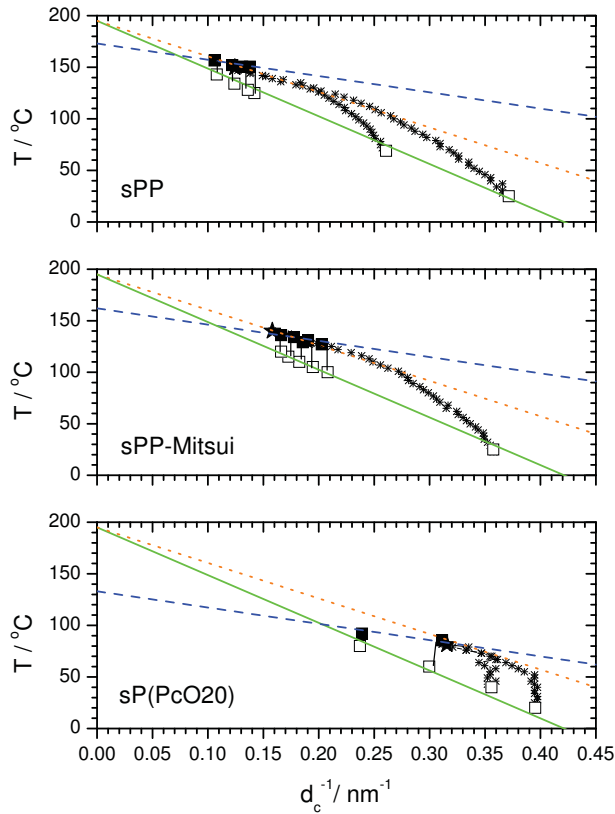
FIG. 13 Three different samples of sPP, crystallized at various temperatures and heated: Inverse crystal thicknesses at the beginning (*open squares*), at melting points (*filled squares*) and at the end point of recrystallization processes(*stars*). All crystallization lines and recrystallization lines (*dots*) are identical, the melting lines (*dashes*) are shifted against each other (Heck *et al.*, 2007).

ends at the same temperature as the crystallization line.

This recrystallization is a rapid process, much faster than the initial crystallization. This was demonstrated by Schick and coworkers (Minakov *et al.*, 2004) in a study of the melting of cold crystallized poly(ethylene terephthalate) with a chip calorimeter which allows heating rates up to 10^5 K min^{-1} for thin films. Only for such high heating rates recrystallization was suppressed in this sample. On the other hand, for sufficiently low heating rates structural changes are well-defined and no longer rate dependent. A step-like sample heating with annealing times in the order of minutes is usually accompanied by a full establishment of new stationary structures.

The described results suggest the validity of a simple scheme for the description of crystallization, recrystallization and melting which can be generally applied to crystallizable polymers and related statistical copolymers. The scheme can be set up using a d_c^{-1}/T-diagram and is presented in Fig. 14 with the data of one of the *s*-polypropylene samples. The diagram is composed of three lines,
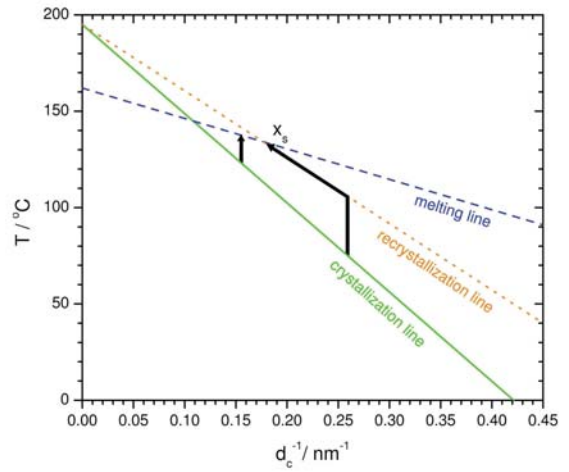

FIG. 14 *General scheme treating crystallization, recrystallization and melting, exemplified with data of sPP. Sample invariant crystallization line and recrystallization line, sample dependent melting line (here: for sPP-Mitsui). Pathways followed during heating processes subsequent to an isothermal crystallization at low temperatures (recrystallization before melting, fixed melting point X_s at the intersection of recrystallization line and melting line) and high temperatures (melting without prior recrystallization).*

- the crystallization line representing the relationship between the crystallization temperature and the inverse crystal thickness d_c^{-1},

- the recrystallization line controlling the course of recrystallization processes,

- the melting line with all final melting points.

Crystallization line and recrystallization line are sample-invariant, i.e., they are not affected by the co-unit content. The melting line, on the other hand, shifts to lower temperatures when the chemical disorder in the chain increases. Melting line and recrystallization line intersect each other at a certain temperature and a certain value of d_c^{-1}. This point of intersection, denoted X_s in Fig. 14 , marks the end of recrystallization processes. If the initial value of the crystal thickness is above the thickness value at X_s no recrystallization occurs; the sample just melts. For an initial thickness below the critical value one has always recrystallization before melting. Whenever the recrystallization line is reached during a heating experiment, d_c^{-1} varies from thereon linearly with T guided by the line, up to the temperature at X_s where the crystals melt. This temperature of final melting varies between different samples according to the displacement of X_s.

B. Granular substructure of lamellar crystallites

The lamellar crystallites have a granular substructure. Evidence is provided by the widths of the $hk0-$Bragg reflections in X-ray scattering patterns, Δq_{hk0}, which are proportional to the inverse of the coherence length along the normal onto the respective lattice plane. Denoting the coherence length D_{hk0}, the relationship is described by the Scherrer equation

$$D_{hk0} = \frac{2\pi}{\Delta q_{hk0}} \quad . \tag{6}$$

For polymers, reflections are much broader than in the case of low molar mass crystals and generally indicate coherence lengths of several to some tens of nanometers. This small coherence length is to be identified with the extension of crystal blocks which compose the lamella. They show up directly in electron micrographs, then, when a staining agent penetrates into the block boundaries (Michler, 1992), and sometimes also in atomic force microscope (AFM) images. The examples presented in Figs. 15 and 16 were obtained for samples of i-polypropylene and s-polypropylene, respectively. The granular structure is clearly apparent, and as we see, the lateral extension of the blocks is comparable to the crystallite thickness. As it turned out, the lateral size of the
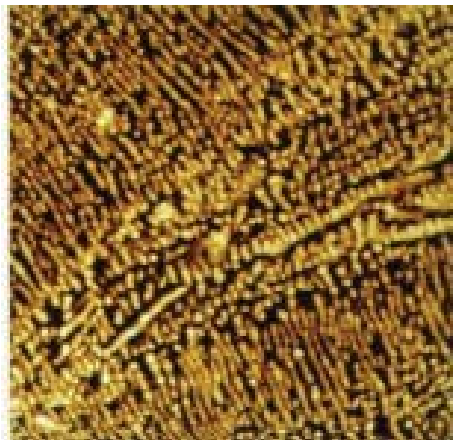

FIG. 16 Sample of sPP: AFM tapping mode image of the edges of up standing crystals showing a granular substructure (scan over 1.25μm in both directions) (Hugel et al., 1999).
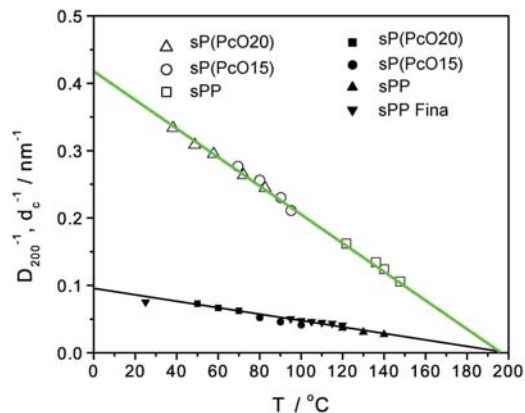
FIG. 17 Different samples of sPP (sPP, sPPcOx and sPP-Fina) crystallized at various temperatures T: Crystallization line d_c^{-1} versus T determined by SAXS (open symbols) and inverse lateral coherence lengths D_{200}^{-1} derived from the linewidth of the 200-reflection (filled symbols) (Hippler et al., 2005).

FIG. 15 Sample of iPP, AFM tapping mode image of lamellar crystallites which stand up, i.e., are oriented with the fold surfaces perpendicular to the image plane. The lines representing the edges of the crystallites are not continuous as in the electron micrograph of Fig. 2 but broken up in small blocks. The image demonstrates that the lamellar crystallites have a granular substructure. Scan over 1μm in both directions obtained by Magonov and Godovsky (Magonov and Godovsky, 1999).

blocks changes with temperature in systematic manner, namely, exactly proportional to the crystal thickness d_c. Fig. 17 presents the temperature dependence of the two lengths d_c and D_{220} as obtained for different samples of s-polypropylene. As can be seen, all points $D_{200}^{-1}(T)$ are allocated on one common line. When continued, this line ends again at $T_c^\infty = 195\ ^\circ\text{C}$, like the crystallization
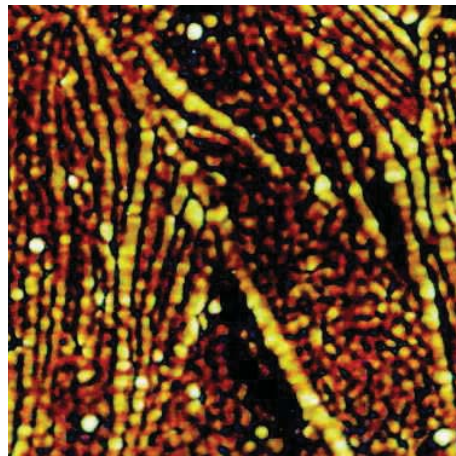
line of s-polypropylene. Analogous results were obtained for polyethylene and related copolymers (Hippler et al., 2005).

C. Zero growth temperature

For many decades it was taken for granted that the growth rate of polymer crystallites is controlled by the supercooling below the equilibrium melting point of a macroscopic sample, T_f^∞, and Eq.(3) of the Hoffman-Lauritzen model was generally used in evaluations of temperature dependent growth rate measurements. Growth rates are controlled by an activation barrier, and the second exponential factor in Eq.(3) states that the height of

this activation barrier diverges at T_{f}^{∞}. In the Hoffman-Lauritzen model this is a consequence of the divergence of both the crystal thickness and the size of the secondary nucleus at T_{f}^{∞}, as described by Eq.(2). The small angle X-ray scattering experiments described in section III.A contradict Eq.(2); the temperature dependence of the crystal thickness is to be described by Eq.(5) which no longer includes T_{f}^{∞}. As a consequence, doubts arouse also with regard to the validity of Eq.(3).

In a first check we carried out growth rate measurements on poly(ϵ-caprolactone). Its crystallization and melting properties were well-characterized by the small angle X-ray scattering experiments. The equilibrium melting point is $T_{\mathrm{f}}^{\infty}=99$ °C , and the temperature controlling the crystal thickness according to Eq. (5) is $T_{\mathrm{c}}^{\infty}=135$ °C (see Fig. 10). The difference between these two temperatures is especially large. In poly(ϵ-caprolactone) a low number of spherulites is slowly growing to large sizes, which is a favorable situation for accurate growth rate measurements in a polarizing optical microscope. The results were already presented, in Fig. 7 , giving growth rates between 47 °C and 58 °C .

Using Eq. (3) means to include as a basic assumption that the activation energy diverges at T_{f}^{∞}. Actually, whether or not this is correct, can be examined by the experiment. One replaces the set parameter T_{f}^{∞} by a variable temperature T_{zg}. A differentiation of $\ln u$ with regard to T and some reordering leads to

$$\left(-\frac{\mathrm{d}\ln(u/u_0)}{\mathrm{d}T}+\frac{T_{\mathrm{A}}^*}{T^2}\right)^{-1/2}=T_{\mathrm{G}}^{-1/2}(T_{\mathrm{zg}}-T) \ . \ (7)$$

Application of this equation allows T_{zg} to be determined; values for T_{A}^* are available in the literature. Fig. 18 presents a plot as suggested by Eq. (7). As is
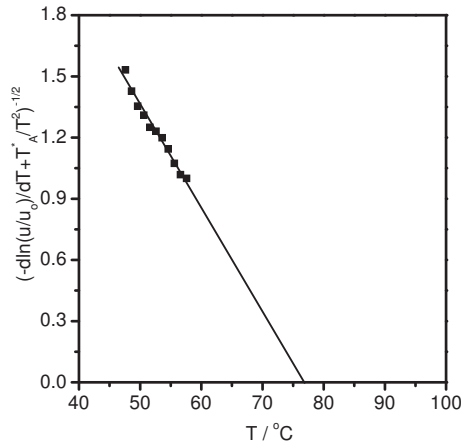

FIG. 18 PϵCL: Temperature dependence of the radial growth rate. Plot based on Eq. (7) giving $T_{\mathrm{zg}}=77$ °C (Cho et al., 2007a).

obvious, the equation can indeed be used for a determination of the 'zero growth temperature' T_{zg}. Data points are all on a straight line, and the extrapolation down to

zero yields T_{zg} with a value of 77 °C . This temperature is far below the equilibrium melting point of 99 °C .

A second check concerned the growth rate of polyethylene. Here the equilibrium melting point is located between 141.4 °C (given by Wunderlich as measured for macroscopic 'extended chain crystals' (Wunderlich, 1980)) and 144.7 °C (derived by Flory and Vrij using an extrapolation of n-alkane melting points (Flory and Vrij, 1963)). Fig. 19 shows data of an own measurement plotted as suggested by Eq.(7). The result for T_{zg} is
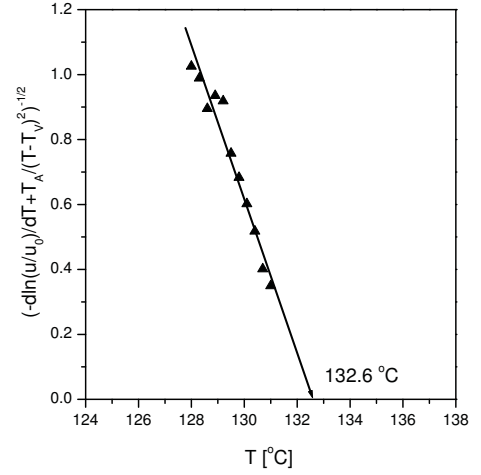

FIG. 19 Growth rates of PE represented according to Eq.(7) (Cho et al., 2007b).

132.6 °C which is again far below the equilibrium melting point.

Hence, the popular, broadly used Eq. (3) is indeed incorrect. The activation energy does not diverge at T_{f}^{∞} but definitely earlier. Obviously Eq. (3) has to be replaced by another relationship, namely

$$u=u_0\exp\left(-\frac{T_{\mathrm{A}}^*}{T}\right)\cdot\exp\left(-\frac{T_{\mathrm{G}}}{T_{\mathrm{zg}}-T}\right) \ . \ (8)$$

It includes T_{zg} as a third temperature characteristic for a given polymer system, different from both T_{f}^{∞} and T_{c}^{∞}.

D. Summary of controlling laws

Thus, as we have seen, experiments revealed that crystallization and melting of polymers in bulk can be described by a number of laws. We summarize them here once again:

- The first law gives the melting point T of plate-like crystallites with thickness d_{c} which is depressed due to the excess free energy of the fold surface. It is expressed by the Gibbs-Thomson equation (1)

$$d_{\mathrm{c}}^{-1}=C_{\mathrm{f}}(T_{\mathrm{f}}^{\infty}-T) \quad \text{with} \quad C_{\mathrm{f}}=\frac{\Delta h_{\mathrm{f}}}{2\sigma_{\mathrm{e}}T_{\mathrm{f}}^{\infty}}.$$

T_{f}^{∞} is the equilibrium melting point of macroscopic crystals. If co-units are incorporated in the chains a further drop of melting points results .

- A second law concerns the relationship between the crystal thickness and the crystallization temperature T. It has also the form of a Gibbs-Thomson equation, but includes another controlling temperature, T_{c}^{∞} (Eq.(5)):

$$d_{\mathrm{c}}^{-1} = C_{\mathrm{c}}(T_{\mathrm{c}}^{\infty} - T) \ .$$

As an important property, Eq.(5) holds commonly for the homopolymer and related statistical copolymers of a system.

- For crystallization temperatures below some characteristic value a subsequent heating leads to continuous recrystallization processes. They follow the recrystallization line given by

$$d_{\mathrm{c}}^{-1} = C_{\mathrm{r}}(T_{\mathrm{c}}^{\infty} - T) \quad . \tag{9}$$

All recrystallized samples melt at the same point, independent of the initial crystallization temperature.

- A further law concerns the temperature dependence of the lateral size of the crystalline blocks which are the constituent elements of the lamellae: The lateral extension of the blocks is proportional to their height in chain direction d_{c}.

- Crystallites grow in lateral direction only, with a rate which increases exponentially with the supercooling below the zero growth temperature T_{zg} as expressed by Eq.(8).

Polymer crystallization and melting processes are thus controlled by three characteristic temperatures, T_{f}^{∞}, T_{c}^{∞} and T_{zg}. They are arranged as

$$T_{\mathrm{zg}} < T_{\mathrm{f}}^{\infty} < T_{\mathrm{c}}^{\infty} \quad .$$

IV. THERMODYNAMICS OF CRYSTAL GROWTH

A. Applying Ostwald's rule of stages

Given this set of experimentally well-founded laws one has to ask about their physical background. What is the reason for the occurrence of three characteristic controlling temperatures ? What is the meaning of the various lines showing up in a T/d_{c}^{-1} diagram ? To begin with, the difference between the crystallization line and the melting line in the macroscopic limiting temperature and in the effect of co-units demonstrates that different laws control

crystallization and melting in bulk polymers. Here, crystallization and melting are not reverse processes. While melting is certainly associated with a direct transfer of chain sequences from lateral crystal faces into the melt, formation of crystals obviously follows another route - very probably one which uses a passage through some intermediate phase. In their crystallization experiments on polyethylene at elevated pressures during the early 1990s, Keller and his co-workers observed a nucleation into a metastable hexagonal phase prior to the transformation into the stable orthorhombic phase (Rastogi *et al.*, 1991) (Keller *et al.*, 1994). They interpreted their observations as an example for Ostwald's rule of stages. This rule, formulated about one hundred years earlier, states that crystals nucleate into that mesomorphic or crystalline structure which is the most stable one for nanometer sized objects (Ostwald, 1897). Due to differences in the surface free energy this state may differ from the macroscopically stable crystal form. Searching for an understanding of polymer crystallization under normal pressure conditions, we felt that Ostwald's rule of stages when applied to the growth process might again provide the clue, and developed a corresponding model.

Indeed, participation of a transient 'mesophase' with a state of order intermediate between the melt and the crystal yields a natural explanation for the existence of three controlling temperatures. These can be identified with the three transition temperatures between the melt, the crystal and the mesophase. The basic conditions under which such a mesomorphic phase can interfere and thus affect the crystallization process are described in the drawing of Fig. 20 . The scheme shows for both the crys-
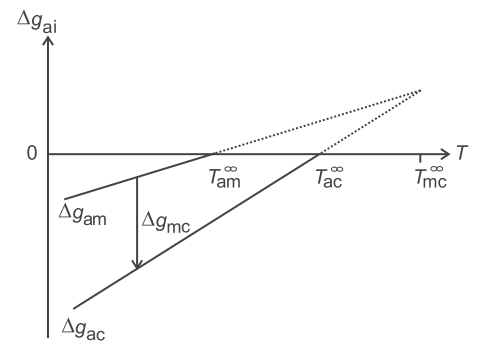

FIG. 20 Thermodynamic conditions assumed for crystallizing polymers : Temperature dependencies of the bulk chemical potentials of a mesomorphic (label m) and the crystalline phase(c). The potentials are referred to the chemical potential of the amorphous melt(a) (Strobl, 2006).

talline phase and the mesomorphic phase the difference of the bulk chemical potential to that of the melt:

$$\begin{aligned} \Delta g_{\mathrm{ac}} &= g_{\mathrm{c}} - g_{\mathrm{a}} \\ \Delta g_{\mathrm{am}} &= g_{\mathrm{m}} - g_{\mathrm{a}} \ . \end{aligned} \tag{10}$$

Coming from high temperatures the chemical potential of the crystalline phase drops below the value of the

melt when crossing the equilibrium melting point T_{ac}^∞. The mesomorphic phase requires a lower temperature to fall with its chemical potential below that of the melt, here named T_{am}^∞. The plot includes also the temperature T_{mc}^∞. It represents the temperature of a virtual transition, namely that between the mesomorphic and the crystalline phase. The three temperatures have the order

$$T_{am}^\infty < T_{ac}^\infty < T_{mc}^\infty \quad . \tag{11}$$

Since the bulk chemical potential of the crystal is always below that of the mesomorphic phase, the mesomorphic phase is only metastable for macroscopic systems. However, for small objects, with sizes in the nanometer range, stabilities can be inverted. Due to a usually lower surface free energy, thin mesomorphic layers can have a lower Gibbs free energy than a crystallite with the same thickness. Then Ostwald's rule of stages applies.

Thermodynamics relates the three transition temperatures T_{am}^∞, T_{ac}^∞, T_{mc}^∞ to the entropy increases $\Delta s_{ma} = s_a - s_m$ and $\Delta s_{ca} = s_a - s_c$ associated with a melting of the mesomorphic and the crystalline phase, respectively. Since the slopes of Δg_{am} and Δg_{ac} are given by Δs_{ma} and Δs_{ca}, one can write in linear approximation

$$(T_{mc}^\infty - T_{ac}^\infty)\Delta s_{ca} \approx (T_{mc}^\infty - T_{am}^\infty)\Delta s_{ma} \tag{12}$$

or

$$\frac{\Delta h_{ma}}{\Delta h_{ca}} = \frac{\Delta s_{ma}T_{am}^\infty}{\Delta s_{ca}T_{ac}^\infty} \approx \frac{(T_{mc}^\infty - T_{ac}^\infty)T_{am}^\infty}{(T_{mc}^\infty - T_{am}^\infty)T_{ac}^\infty} \quad . \tag{13}$$

B. Multistage model and nanophase diagram

A possible pathway for the growth of polymer crystallites mediated by a mesophase is shown in Fig. 21 . In

stabilization by surface ordering   solidification by core crystallization   growing mesomorphic layer
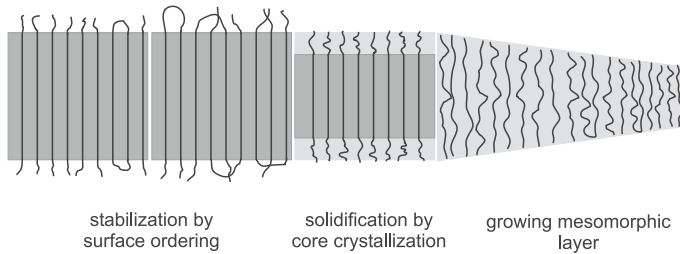
FIG. 21 Multistage model of polymer crystal growth. Rather than being directly attached to the crystal surface chain segments of the melt are first incorporated in a thin layer with mesomorphic structure in front of the crystallite. The mesomorphic layer thickens spontaneously. When reaching a critical thickness a crystal block forms by a first order transition. In a last step the excess energy of the fold surface is reduced (Strobl, 2007).

this multistage model crystal growth proceeds in several steps. A thin layer with mesomorphic inner structure

forms between the lateral crystal face and the melt, stabilized by epitaxial forces. All the co-units are already rejected on its front. A high inner mobility allows a spontaneous thickening of the layer up to a critical value where the core region crystallizes under formation of a block. In a last step the surface region of this block, at first still disordered, perfects, which leads to a further stabilization. Based on this model it is possible to construct a thermodynamic scheme which shows all the features of Fig. 14 , i.e., a crystallization line, a recrystallization line and a melting line. It deals with four different phases:

- the melt

- mesomorphic layers

and two limiting forms of the crystallites, namely

- native crystals (labeled 'c$_n$') and

- stabilized crystals (with label 'c$_s$').

The scheme, being displayed in Fig. 22 , delineates the stability ranges and transition lines for these phases. The
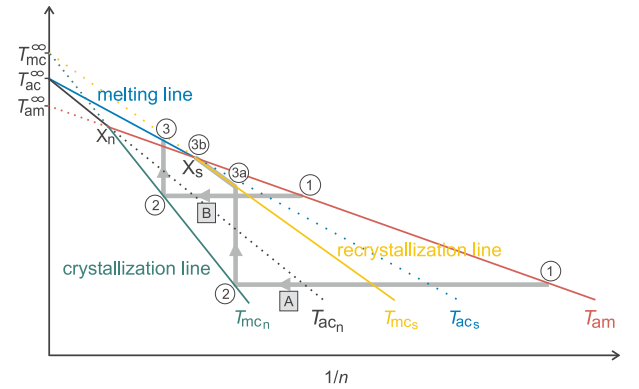
FIG. 22 T/n^{-1} phase diagram for polymer layers in a melt (label a) dealing with three phases: mesomorphic (m), native crystalline (c$_n$) and stabilized crystalline (c$_s$). Lines of size dependent phase transitions: T_{mc_n} between mesomorphic and native crystalline layers, T_{ac_n}, T_{mc_s}, T_{ac_s}, T_{am} with corresponding meanings. Two routes for an isothermal crystallization followed by heating: route A for low crystallization temperatures and route B for high crystallization temperatures. Triple points X$_n$ / X$_s$ with coinciding Gibbs free energies of the melt, a mesomorphic layer and a native / stabilized crystalline layer with the same thickness (Strobl, 2006).

variables in this phase diagram are the same ones as in Fig. 14 , i.e. the temperature and the inverse crystal thickness, the latter being given by the number n of structure units in a stem,

$$n = \frac{d_c}{\Delta z} \quad \text{with } \Delta z \text{ denoting the length per structure unit.}$$

Application of the model implies to interpret the three lines in Fig. 14 as transition lines in a T/d_c^{-1} phase diagram, identifying

- the line named T_{ac_s} with the melting line ($T_{ac}^\infty = T_f^\infty$)

- the line T_{mc_n} with the crystallization line, which implies in particular that T_c^∞, the controlling temperature for the crystal thickness, is set equal to the transition temperature T_{mc}^∞.

- line T_{mc_s} with the recrystallization line.

The Gibbs-Thomson equation generally deals with the effect of surface free energies on transition temperatures. It can not only be applied to lamellar crystallites but in analogous manner also to temperature and size dependent transitions of layers with mesomorphic structure. This leads for the crystallization line to the theoretical expression

$$T_c^\infty - T \approx \frac{(2\sigma_{ac_n} - 2\sigma_{am})T_c^\infty}{\Delta h_{cm}} \frac{1}{n} \qquad (14)$$

and for the recrystallization line to

$$T_c^\infty - T \approx \frac{(2\sigma_{ac_s} - 2\sigma_{am})T_c^\infty}{\Delta h_{cm}} \frac{1}{n} \quad . \qquad (15)$$

σ_{am} and σ_{ac_n} denote the surface free energy of the mesomorphic layer and the native crystal layer, respectively. The surface free energy of the stabilized crystallites denoted σ_e in Eq.(1) is renamed as σ_{ac_s}.

The thermodynamic scheme associated with the model includes as a further line the stability limit T_{am} of layers with mesomorphic structure which starts from the macroscopic transition temperature T_{am}^∞. The Gibbs-Thomson equation yields for this case

$$T_{am}^\infty - T \approx \frac{2\sigma_{am}T_{am}^\infty}{\Delta h_{ma}} \frac{1}{n} \quad . \qquad (16)$$

For temperatures above T_{am}^∞ the mesophase no longer exists. The mesophase mediated growth process assumed by the multistage model here comes to an end. This, however, is exactly the property of the zero growth temperature. Hence, we identify T_{zg} with T_{am}^∞. Note that the ordering of the limiting temperatures in the model (Eq.(11)) agrees with the observations

$$T_{zg} = T_{am}^\infty < T_f^\infty = T_{ac}^\infty < T_c^\infty = T_{mc}^\infty \quad .$$

Of particular importance in the 'nanophase diagram' of Fig. 22 are the triple points X_n and X_s. At X_n both mesomorphic layers and native crystals have the same Gibbs free energy as the melt, at X_s this equality holds for the stabilized crystallites. The positions of X_n and X_s control what happens during an isothermal crystallization followed by heating. In agreement with the experiments the scheme predicts two different scenarios exemplified by the routes A and B. Route B, realized by crystallizations at high temperatures, is as follows: At the point of entry, labelled '1', chains are attached from the melt onto the front of a mesomorphic layer with minimum

thickness. The layer spontaneously thickens until the transition line T_{mc_n} is reached at point '2', where native crystals form immediately. The subsequently following stabilization transforms them into a lower free energy state, and the crossing point is shifted to X_s. On heating crystallites remain stable up to the transition line T_{ac_s} associated with a melting of the crystal. Route A (low crystallization temperatures) is different: The beginning is the same - starting at point 1 with an attachment of chain sequences onto a spontaneously thickening mesomorphic layer, then, on reaching T_{mc_n}, the formation of native crystals followed by a stabilization. When heating the stabilized crystals they at first retain their structure. However, now at first the transition line T_{mc_s} is met which relates to a transformation into the mesomorphic state instead of melting. The consequence for a further heating is a continuous recrystallization mediated by the mesophase ((3a) to (3b)). This ends at the triple point X_s where the crystal melts.

What is the nature of the temperature dependent activation barrier showing up in the second exponential factor in Eq.(8) determining the growth rate? The proposed multistage model includes a possible answer. The series of steps sketched in Fig. 21 involves several activation barriers. The first step - attachment of a chain sequence on the growth front of the mesomorphic layer - could be dominant, and the observations support this supposition. Before a sequence, which lies coiled in the melt, is incorporated into the growing mesomorphic layer, it has to be 'activated' by a transfer into an overall straightened form as required for an attachment. The straightening has to reach at least the length given by the initial thickness of the mesomorphic layer. The number of monomers in such a sequence, n^*, is determined by Eq.(16), as

$$n^* = \frac{2\sigma_{am}T_{am}^\infty}{\Delta h_{ma}} \frac{1}{T_{am}^\infty - T} \quad . \qquad (17)$$

Since the straightening leads to a decrease in entropy which is proportional to the sequence length it introduces an entropic activation barrier

$$-\frac{\Delta S}{k} \propto n^* \quad . \qquad (18)$$

Transition of the barrier takes place with a probability

$$\exp\frac{\Delta S}{k} = \exp-\frac{\text{const}}{T_{am}^\infty - T} \quad . \qquad (19)$$

Since we identify T_{am}^∞ with T_{zg}, the theoretical expression agrees with the experimental result as given by Eq.(8).

C. Model based data evaluation

Application of the scheme to experimental results, as given by the crystallization line, the melting line, the recrystallization line of a system and the zero growth rate temperature yields the thermodynamic parameters

included in the equilibrium relationships. Fig. 23 shows once again the data of poly(ϵ-caprolactone) from Fig. 10 , now complemented by the recrystallization line and the a⇒m transition line. The latter is fixed by T_{am}^{∞} ($= T_{\mathrm{zg}}$)
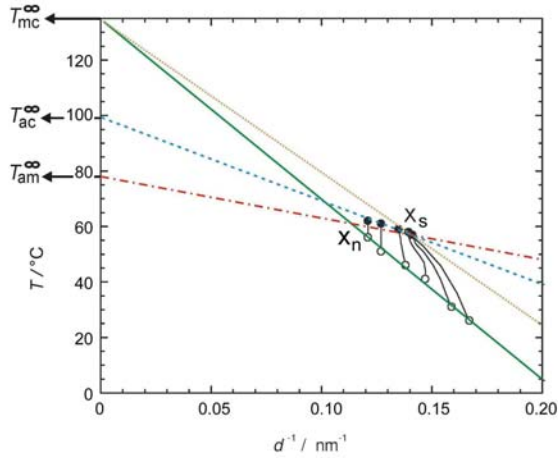

FIG. 23 PϵCL: Crystallization line (*continuous*), recrystallization line (*dots*) and melting line (*dashes*) determined by SAXS, zero growth rate temperature T_{am}^{∞} (from Fig. 18) and a⇒m transition line passing through T_{am}^{∞} and X_{s} (*dash-dots*) (Strobl, 2007).

and the location of X_{s}.

Evaluation of such a nanophase diagram yields

- the enthalpy change Δh_{ma} between the mesomorphic and the amorphous phase

- the surface free energy of mesomorphic lamellae σ_{am}

- the surface free energy of crystalline lamellae in the initial native state, $\sigma_{\mathrm{ac_n}}$

- the surface free energy of crystalline lamellae in the final stabilized state, $\sigma_{\mathrm{ac_s}}$.

The heat of fusion, Δh_{ca}, is usually available in the literature or can be determined by calorimetry. The heat of transition Δh_{ma} then follows from an application of Eq.(13). In the next step σ_{am} is calculated using Eq.(16). The surface free energy $\sigma_{\mathrm{ac_n}}$ is obtained using Eq.(14) with $\Delta h_{\mathrm{cm}} = \Delta h_{\mathrm{ca}} - \Delta h_{\mathrm{ma}}$. The surface free energy of the stabilized crystallites can be calculated applying the corresponding relation Eq.(15).

The data derived in this way for poly(ϵ-caprolactone) from the nanophase diagram in Fig. 23 are collected in Table I.

The heat of transition Δh_{ma} is indicative for a truly intermediate character of the mesomorphic phase, being neither near to the liquid nor resembling a perturbed crystallite. Comparing mesomorphic with crystalline lamellae, the drop of the surface free energy, from

TABLE I PϵCL: Thermodynamic data derived from the experiments

T_{mc}^{∞} $^\circ$C	T_{ac}^{∞} $^\circ$C	T_{am}^{∞} $^\circ$C	Δh_{ca} $\frac{\mathrm{kJ}}{\mathrm{mol}\ C_6H_{10}O_2}$	Δh_{ma} $\frac{\mathrm{kJ}}{\mathrm{mol}\ C_6H_{10}O_2}$	$\sigma_{\mathrm{ac_n}}$ $\frac{\mathrm{kJ}}{\mathrm{mol}}$	$\sigma_{\mathrm{ac_s}}$ $\frac{\mathrm{kJ}}{\mathrm{mol}}$	σ_{am} $\frac{\mathrm{kJ}}{\mathrm{mol}}$
135	99	78	17.9	11.4	9.7	8.4	2.5

$\sigma_{\mathrm{ac_n}}$ and $\sigma_{\mathrm{ac_s}}$ to σ_{am}, is larger than that in the heat of transition from Δh_{ca} to Δh_{ma}. This is, indeed, an expected result. Only under this condition stabilities of crystalline and mesomorphic lamellae become inverted for nanocrystallites, thus opening the mesophase mediated growth route.

With the a⇒m transition line also the triple point X_{n} is fixed, being located at the intersection with the crystallization line. The point X_{n} marks the respective end of the mesophase-mediated growth process. For crystallization temperatures above $T(X_{\mathrm{n}})$ and crystal thicknesses above $d(X_{\mathrm{n}})$ growth must proceed by a direct attachment of chain sequences onto the lateral growth face of the crystal. As it appears, so far experiments never entered this temperature range. In principle, polymers also crystallize between $T(X_{\mathrm{n}})$ and T_{ac}^{∞}, however, as it seems, this occurs with a vanishingly low rate. For the observed practically realized crystallization rates the participation of an intermediate mesomorphic phase is obviously a necessity.

V. FINAL REMARKS

In the field of polymer crystallization we are presently in a time of shifting paradigmas away from conventional wisdom, but it will need more years to establish a generally accepted new understanding. The experimental results presented in this article provide a sound basis. They can be expressed by some equations of simple form which relate the thickness and growth rate of the plate-like crystallites in polymeric solids to the supercooling below two characteristic temperatures. Since both differ from the equilibrium melting point their existence invalidated the long accepted Hoffman-Lauritzen model. The findings, resulting from temperature dependent structural studies using X-ray scattering and optical microscopy, ask for a comprehensive explanation. The existence of three different controlling temperatures rather than a unique one is - in our view - indicative for the participation of a third transient phase in the growth process, and we developed a corresponding theoretical model on thermodynamics grounds. The response in the polymer physics community varies; we don't see a blunt rejection but full acceptance is also rare. Of course, we hope that our view finally will be accepted as the correct concept, but are aware that this time has not yet come. Convincing the whole community would be much facilitated if the proposed presence of a small region with mesomorphic

structure at the front of a growing lamellar crystallite could be shown directly, rather than inferring it from the laws which govern crystallization and melting. Atomic force microscopy with its high spatial resolution has the potential to realize this aim, however, so far an image with the character of the multistage model sketched in Fig. 21 has not been reported. The reason could be that the mesomorphic phase is passed through very rapidly, maybe even in the manner that it exists as a transient state during the formation of a block only. The block formation would then resemble the formation of a nucleus, and the building of a crystal lamella consequently a repeated self-supported and guided nucleation. That crystal nucleation can be accelerated by a passage through an intermediate phase is known since Ostwald's time, and it is corroborated by convincing experiments, for example, by the nucleation studies on *n*-alkanes carried out by Sirota et al (Sirota and Herhold, 1999). There could, however, also be another reason for the non-visibility of the mesomorphic phase in the AFM studies: Its surface stiffness could be near to that of the crystal so that the contrast would be insufficient to show up in the images. Li et al (Li *et al.*, 2001) reported in one work a certain weakness of the front zone of growing polyester lamellae and related it to perturbations of the crystal structure.

The necessary revision of the traditional views about the crystallization in bulk polymer melts has revived the debate in the whole field after a longer period with reduced interest. There are several further issues, new and traditional ones, some of them of great technical importance, which are now intensely discussed at general conferences and focussed meetings (see, for example, the Lecture Notes of the last EPS Discussion Meeting in Waldau (Reiter and Strobl, 2007)). These are, in particular,

- primary nucleation phenomena

- long living structures in the melt affecting the crystallization process

- confinement effects on crystallization as they are found, for example, in block copolymers

- crystallization in flowing melts with oriented chains, or

- mobility restrictions in the regions near to crystallites.

Conditions in polymeric systems are peculiar and different from other materials. Experiments on polymeric systems therefore always require special tools for the preparation or the data evaluation and need special approaches in theoretical treatments or computer simulations. For a long period polymer physics played only a side role in teaching and research programs of physics departments, if it was included at all . With the uprise of biophysics, organic electronics and the various uses of soft matter the situation has changed. Polymer physics provides the basis, and polymer crystallization is here a central phenomenon.

References

Cho, T., W. Stille, and G. Strobl, 2007a, Colloid Polym Sci **285**, 931.

Cho, T., W. Stille, and G. Strobl, 2007b, Macromolecules **40**, 2590.

Eppe, R., E. Fischer, and H. Stuart, 1959, J.Polym.Sci. **34**, 721.

Faraday-Discussion, 1979, Faraday Disc.Chem.Soc. **68**.

Flory, P., and A. Vrij, 1963, J.Am.Chem.Soc. **85**, 3548.

Hauser, G., J. Schmidtke, and G. Strobl, 1998, Macromolecules **31**, 6250.

Heck, B., T. Hugel, M. Iijima, E. Sadiku, and G. Strobl, 1999, New J.Physics **1**, 17.

Heck, B., S. Siegenfuehr, G. Strobl, and R. Thomann, 2007, Polymer **48**, 1352.

Hippler, T., S. Jiang, and G. Strobl, 2005, Macromolecules **38**, 9396.

Hoffman, J., G. Davis, and J. Lauritzen, 1976, in *Treatise on Solid State Chemistry* Vol.3, N.B.Hannay Ed. (Plenum), p. 497.

Hugel, T., G. Strobl, and R. Thomann, 1999, Acta Polym. **50**, 214.

Imai, M., K. Kaji, T. Kanaya, and Y. Sakai, 1995, Phys. Rev. B **52**, 12696.

Kanig, G., 1975, Progr.Colloid Polym.Sci. **57**, 176.

Keller, A., M. Hikosaka, S. Rastogi, A. Toda, P. Barham, and G. Goldbeck-Wood, 1994, J.Mater.Sci. **29**, 2579.

Li, C., L.and Chan, K. Yeung, and K. L. Y. Li, J.X.and Ng, 2001, Macromolecules **34**, 316.

Magonov, S., and Y. Godovsky, 1999, American Laboratory **31**, 55.

Michler, G., 1992, *Kunststoff-Mikromechanik* (Carl Hanser Verlag), p. 187.

Minakov, A., D. Mordvintsev, and C. Schick, 2004, Polymer **45**, 3755.

Olmsted, P., W. Poon, T. McLeish, T. Terrill, and A. Ryan, 1998, Phys. Rev. Lett. **81**, 373.

Ostwald, W., 1897, Z.Phys.Chem. **22**, 286.

Rastogi, S., M. Hikosaka, H. Kawabata, and A. Keller, 1991, Macromolecules **24**, 6384.

Reiter, G., and G. Strobl, 2007, *Progress in Understanding of Polymer Crystallization. Lecture Notes in Physics 714*

(Springer).

Ruland, W., 1977, Colloid Polym.Sci. **255**, 417.

Schmidtke, J., G. Strobl, and T. Thurn-Albrecht, 1997, Macromolecules **30**, 5804.

Sirota, E., and A. Herhold, 1999, Science **283**, 529.

Strobl, G., 2000, Eur.Phys.J.E **3**, 165.

Strobl, G., 2006, Progr.Polym.Sci. **31**, 398.

Strobl, G., 2007, *The Physics of Polymers. 3rd Edition* (Springer), p. 165.

Vaughan, A., and D. Bassett, 1989, *Comprehensive Polymer Science, Vol.2* (Pergamon Press), p. 415.

Wunderlich, B., 1980, *Macromolecular Physics, Volume 3* (Academic Press), p. 58.